Pozuelo, J., Mendicuti, F. & Mattice, W. L. (1997): Inclusion Complexes of Chain Molecules with Cycloamyloses. 2. Molecular Dynamics Simulations of Polyrotaxanes Formed by Poly(ethylene glycol) and α-Cyclodextrins. *Macromolecules*, 30 (12), pp.: 3685–3690.

Inclusion Complexes of Chain Molecules with Cycloamyloses. 2. Molecular Dynamics Simulations of Polyrotaxanes Formed by Poly(ethylene glycol) and • -Cyclodextrins

Javier Pozuelo, Francisco Mendicuti, and Wayne L. Mattice*

Departamento de Química Física, Universidad de Alcalâ, 28871 Alcalá de Henares, Madrid, Spain, and Institute of Polymer Science, The University of Akron, Akron, Ohio 44325-3909

ABSTRACT: Molecular dynamics (MD) simulations were performed for "channel type" polyrotaxanes with • -cyclodextrins (• -CDs) threaded onto monodisperse chains of poly(ethylene glycol) (PEG). The polymer captures as much • -CD as its length permits, forming a close-packed structure from the one end to the other. The van der Waals interactions are the main source of the stabilization of these polyrotaxanes. Hydrogen bonds between successive • -CDs slightly favor head-to-head, tail-to-tail sequences over head-to-tail sequences. The • -CDs in polyrotaxanes are more symmetric and less distorted than the isolated • -CDs. The PEG in the polyrotaxane is more extended than an unperturbed chain, because it has a larger population of *trans* states at internal bonds.

Introduction

Cyclodextrins (CDs) are macrocycles formed by six or more glucose units connected by • -1,4-linkages. The best known, with six to nine glucose units, are named • -(6), • -(7), • -(8), and • -(9) CD. The CDs form inclusion complexes with various compounds of low molecular weight.[1• 3] The importance of noncovalent interactions in host• guest complexes in biological systems motivates the current interest in supramolecular assemblies[4] because of their unique structures and properties.[5] A rotaxane is a classic example of a supermolecule in which a molecular "rotor" is threaded by a linear "axle". This molecular assembly may be important in the creation of molecular tubes and molecular devices. Earlier examples include crown ethers threaded by polymers[6] and CD complexes.[7• 13]

Recently Harada and co-workers prepared polyrotaxanes from several polymers and CDs.[14• 20] They obtained complexes between • -CD and poly(ethylene glycol) (PEG) with molecular weight in the range 400• 10 000, but they could not prepare polyrotaxanes with • -CD and the lower molecular weight analogs ethylene glycol, diethylene glycol, and triethylene glycol.[14,16,17] • -CD did not form complexes with PEG of any molecular weight.[18] The ^{13}C CP/MAS NMR spectrum and X-ray of the • -CD• PEG complex suggest that the chain is included in a channel formed by the CDs, producing the "channel type" inclusion complex described by McMullan *et al*.[21] Polyrotaxanes with • - and • -CDs and poly(propylene glycol) (PPG) of various molecular weights were also prepared in high yields, but complexes with low molecular weight analogues were not obtained.[15] • -CD did not form complexes with PPG of any molecular weight.[15] In general, a high selectivity was observed in the formation of polyrotaxanes.[15,18,20] Yields depend strongly on the nature and molecular weight of the polymer.

Most polyrotaxanes formed by • -CD and PEG were synthesized by Harada's group starting from polydisperse polymers, giving heterogeneous rotaxanes. Recently they synthesized and characterized a homogeneous polyrotaxane from monodisperse amino-terminated PEG with a molecular weight of 1248 (28 monomer units).[19] After spontaneous formation of the polyrotaxane in solution, the CDs were trapped by capping the ends of the chain with bulky substituents.[19] Using a variety of techniques, including molecular weight determination and spectroscopy, they find 12 • -CDs in this polyrotaxane, giving approximately 2.3 oxyethylene units per • -CD. Microcalorimetry of the complex indicates hydrogen bond formation between CDs that suggests they assemble in a head-to-head, tail-to-tail sequence.[16] X-ray studies on a single crystal of the complex between • -CD and *p*-nitroacetanilide support this conclusion.[20] Comparison of ^{13}C CP/MAS NMR spectra and X-ray studies of single crystals of • -CD and the • -CD• PEG complex indicates • -CD assumes a more symmetric conformation when it includes a guest in the cavity with each glucose unit in a similar environment.[15,17,18]

Molecular dynamics (MD) simulations have been used to study the conformation and mobility of other systems in which a polymer is confined in a narrow channel. The inclusion compounds of polyethylene,[22• 24] poly(1,4-*trans*-butadiene),[25,26] and poly(1,4-*trans*-isoprene)[27] in perhydrotriphenylene and polyethylene in urea[28] are examples. Static methods have also been used to determine which chain conformations are candidates for inclusion in narrow channels.[29] Here we employ MD simulations of end-capped complexes of • -CDs with PEG, with the focus on polyrotaxanes formed by 8 or 10 oxyethylene units and 3 or 4 • -CDs, giving 2.6 • 0.1 oxyethylene units per CD. Our purpose is not to investigate the internal dynamics, but instead it is to infer the stabilities and configurations of the complexes from the conformations in the trajectory. The parameters that characterize the complex were compared with those obtained for isolated • -CD[30] and an isolated chain of PEG.

Methodology for the Simulations

Molecular dynamics trajectories were computed using Sybyl 6.0 from Tripos Associates (St. Louis, MO) and the Tripos Force Field 5.2.[31] The properties of the isolated • -CDs, evaluated using this same force field, have been reported recently.[30] The molecules studied in the present work were mainly isolated

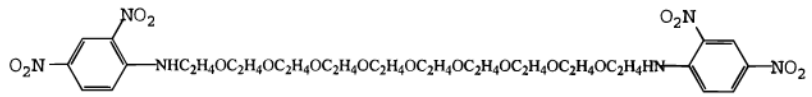

PEG10

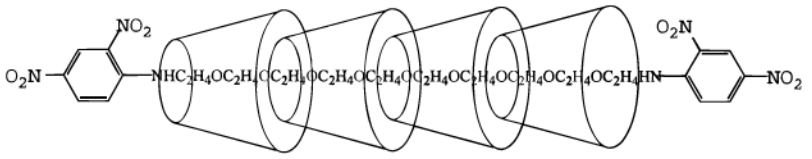

RPEG10CD4HT

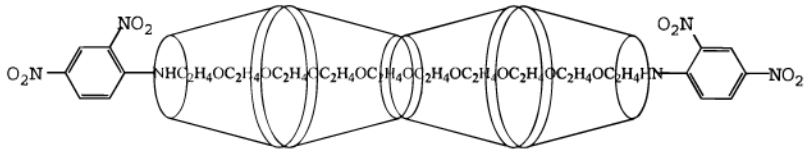

RPEG10CD4HH

Figure 1. An isolated chain containing 10 oxyethylene units (PEG10) and polyrotaxanes containing 10 oxyethylene units and 4 • -cyclodextrins (represented by toruses) oriented head-to-tail (RPEG10CD4HT) or head-to-head and tail-to-tail (RPEG10CD4HH). All PEG are end-capped by 2,4-dinitrophenylamine groups.

chains containing 8 or 10 oxyethylene units and complexes between these chains and 3 or 4 • -CDs, respectively. Henceforth CD denotes • -CD, and isolated chains are abbreviated as PEG*n*, where *n* is the number of oxyethylene units. Polyrotaxanes are abbreviated as RPEG*n*CD*m*, where *m* is the number of CD units. Head-to-head, tail to tail (HH), and head-to-tail (HT) sequences of CDs were distinguished. As with the polyrotaxanes of PEG and CDs synthesized by Harada's group,[19] the polyrotaxanes and PEGs used in the MD simulations were capped at both ends with 2,4-dinitrophenylamine groups. Figure 1 depicts isolated PEG10 and the polyrotaxanes named RPEG10CD4HT and RPEG10CD4HH. Following the usual nomenclature for CDs, the *trans* conformation was defined as 0° for internal bonds in PEG chains.

Bonds connected to hydrogen atoms were constrained in their lengths, but all other bond lengths, bond angles, and torsional angles were variable during the simulations. Electrostatic interactions were taken into account, using pairwise contributions of $q_i q_j / 3.5 r_{ij}$, where r_{ij} is the separation of partial charges q_i and q_j. Following the previous work of Brant and Flory in the conformational analysis of polypeptides[32,33] and polysaccharides,[34] we have used a value of 3.5 for the dielectric constant in the calculation of the electrostatic contribution to the conformational energies. This value provides theoretical conformational energy surfaces that predict theoretical characteristic ratios that are in excellent agreement with those deduced from experiments performed for amylose[35] and polypeptides[36,37] in dilute aqueous solution. Partial charges for PEG*n* and CD as isolated molecules and polyrotaxanes were obtained by MOPAC.[38] A model compound containing four oxyethylene units, terminated with hydroxyl at one end and 2,4-dinitrophenylamine at the other end, was used to calculate the geometry and charges for PEG*n*. As in the study of isolated CDs,[30] geometry and charges for CD were obtained from the central unit of a linear amylose trimer. Partial charges and geometry used for PEG*n* are collected in Table 1, using the numbering scheme defined in the top of Figure 2. The stabilization of the complexes in the simulation is insensitive to the details of the treatment of the electrostatic interactions. Typically the contribution to the binding energy from the electrostatic energy is only 1• 3% of the contribution from the van der Waals interactions.

The bottom of Figure 2 depicts the three dihedral angles •$_{1x}$ (O• CH_2• CH_2• O), •$_{2x}$ (CH_2• CH_2• O• CH_2), and •$_{3x}$ (CH_2• O• CH_2• CH_2) at oxyethylene unit *x*, used to define the conformation of the PEG chains. Initially PEG chains were built with all torsional angles in the *trans* state. CD starting conformations were constructed in the nondistorted form, as previously,[30] with the torsional angles • [at C(4)• C(1)• O• C(4′)] and • [at C(1)• O• C(4′)• C(1′)] at the bonds to the bridging oxygen atom set at 0° and • 3°, respectively, and a value of 130.3° for the bond angle (•) at the bridging oxygen atom. Dihedral angles • for C(4)• C(5)• C(6)• O were set to the *trans* conformation. Starting polyrotaxanes were built placing *m* nondistorted CDs, with centers separated by 7 Å, around the *all-trans* PEG*n* chain.

Table 1. Length, Angles, and Partial Charges in the Poly(ethylene Glycol)s

bond	length, Å	bonds	angle, deg	atom[a]	charge, ecu
C^{ar}• NO_2	1.350	C^{ar}• C^{ar}• C^{ar}	120.00	C1	0.132
N• O	1.210	C^{ar}• C^{ar}• N	120.00	C2	• 0.205
C^{ar}• C^{ar}	1.398	C^{ar}• C^{ar}• NH	120.00	C3	0.049
C^{ar}• NH	1.410	C^{ar}• N• CH_2	109.47	C4	• 0.204
N• CH_2	1.470	CH_2• CH_2• O	109.47	C5	0.020
CH_2• CH_2	1.540	CH_2• O• CH_2	109.47	C6	• 0.224
CH_2• O	1.430	N• CH_2• CH_2	109.47	C7	• 0.108
C^{ar}• H	1.085			C8	• 0.024
C• H	1.103			C9	• 0.023
N• H	1.083			C10	• 0.020
				N (NO_2)	0.593
				N3	• 0.200
				O (NO_2)	• 0.365
				O5	• 0.275
				O6	• 0.028

[a] Charges for hydrogen atoms (not tabulated) produce a neutral PEG chain.

Calculations were performed in a canonical ensemble where *N*, *V*, and *T* were fixed. From 0 K the temperature was increased 10 K at intervals of 300 fs, and the molecule was equilibrated at the final temperature (500 K) for up to 100 ps before the collection of data was initiated. Velocities were rescaled at intervals of 10 fs, and the linear and angular momentum of the entire system was reset to zero at the same interval. The duration of the trajectory was 0.5 ns, computed with a time step of 2 fs using a modification of the Verlet algorithm,[39,40] named the leap from algorithm.[41] Conformations were saved at intervals of 200 fs, yielding 2500 images from each simulation for subsequent analysis. The average

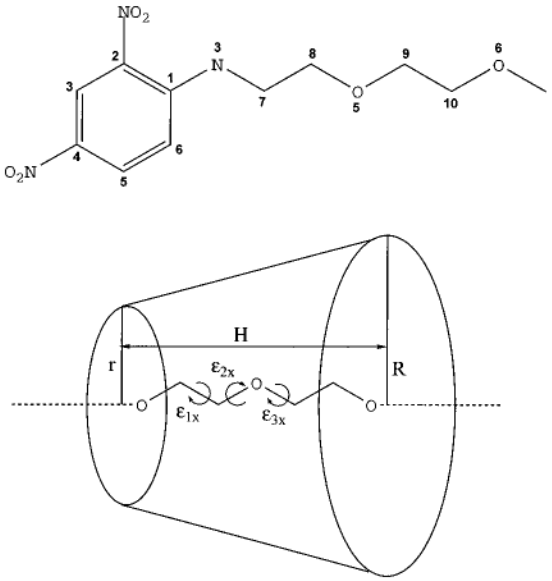

Figure 2. Numbering scheme used for the partial charges, followed by the internal dihedral angles •1, •2, and •3, used to define the conformation of the oxyethylene units in the PEG chain, and three parameters *H*, *R*, and *r*, used to define the size and shape of CD units.

of any property ⟨*X*⟩ was obtained as

$$\langle X \rangle \bullet \ (1/N)\sum X_i \qquad (1)$$

where *N* is the number of images under analysis (2500) and X_i is the value of the property for image *i*.

The potential energy of each image is evaluated as a sum of five contributions,

$$E_{tor} \bullet \ E_{stretch} \bullet \ E_{bend} \bullet \ E_{tors} \bullet \ E_{vdW} \bullet \ E_{ele} \qquad (2)$$

where the terms on the right hand side represent the contributions from bond stretching, bond angle bending, torsion, van der Waals, and electrostatic interactions. For each conformation of RPEG*n*CD*m*, the nonbonded interaction between the PEG chain and CDs or binding energy ($E_{binding}$) was evaluated as the difference between the total energy and the energy of the PEG chain and *m* CD units as

$$E_{binding} \bullet \ E_{RPEGnCDm} \bullet \ (E_{PEGn} \bullet \ E_{CDm}) \qquad (3)$$

The term $E_{RPEGnCDm}$ represents the total potential energy of the complex, and E_{PEGn} and E_{CDm} are the potential energy of the system taking into account only the atoms of PEG*n* or *m* CDs, respectively. Contributions from solvation were ignored in the simulations, which were performed in vacuo. The experimental system experiences a variety of environments during its preparation.[19] The polyrotaxane is initially prepared in an aqueous solution, then dried under vacuum, and finally dissolved in dimethylformamide for the end-capping reaction.[19]

For evaluating the number of intra- and intermolecular hydrogen bonds of *m* CD, a hydrogen bond is assumed when the acceptor and hydrogen bonded to a donor are separated by 0.8• 2.8 Å and the angle formed by O•••H• O is 120°• 180°.

Results and Discussion

1. Stability of the Complexes when Changing the Number of CDs, *m*. MD simulations were performed on RPEG10CD*m*HT with *m* in the range 2• 5. Figure 3 depicts the negative values of $E_{binding}$ as a function of *m*. The $E_{binding}$ values show that a stabilization of the complex occurs as *m* increases from 2 to 4, but for *m* • 5, the stability of the complex decreases. The van der Waals interactions make the dominant contribution to $E_{binding}$, with the electrostatic interactions contributing only 1• 3%. We interpret the initial negative slope in Figure 3 as signifying that the interaction of one bound CD with its bound neighbor contributes to the stabilization of the complex. For this reason, continued incorporation of additional CDs is favored until the capacity of the chain has been saturated. The strong increase in potential energy for PEG• CD*m* when adding a fifth CD comes from its mandatory repulsive interaction with the bulky end groups, due to saturation of that portion of the chain removed from the end groups. The minimum of $E_{binding}$ for PEG• CD*m* at *m* • 4 implies a preferred stoichiometric composition near 2.5 oxyethylene units per CD, which is similar to Harada's experimental result.[19] Since *m* is not a continuous variable, but must instead assume integer values, the result in Figure 3 should be interpreted conservatively as showing the preferred composition is more than 2, but less than 3.3, oxyethylene units per CD.

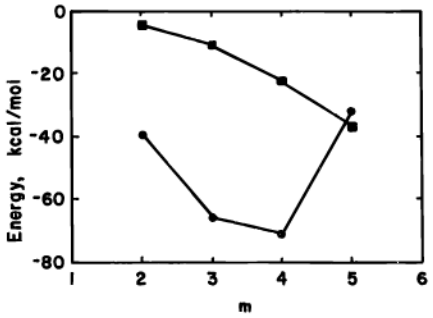

Figure 3. Binding energies for RPEG10CD*m*HT (circles) and that portion of the binding energy that arises from interaction of the CDs with one another (squares).

Table 2. Average Numbers of Intramolecular Hydrogen Bonds (HB) for Each CD, Intermolecular HB between Each Neighboring Pair of CDs, and Number of Intermolecular HB of the Types PEG• CDs and PEG• end group

hydrogen bond	RPEG10CD4HT[a]	RPEG10CD4HH[a]
intra-HB CD1	2.0(1.2)	2.1(1.3)
intra-HB CD2	2.0(1.3)	1.9(1.3)
intra-HB CD3	1.9(1.3)	1.8(1.2)
intra-HB CD4	2.0(1.3)	2.0(1.3)
total intra-HB CDs	8.0(2.6)	7.8(2.5)
inter-HB CD12	1.2(1.1)	2.5(1.7)
inter-HB CD23	1.2(1.1)	0.6(0.8)
inter-HB CD34	1.3(1.1)	2.7(1.7)
total inter CD• CD	3.7(2.0)	5.8(2.5)
total inter CD• PEG	0.4(1.6)	0.4(0.6)
total inter CD• end groups	1.2(1.1)	0.9(1.0)

[a] Standard deviations are in parenthesis.

The remainder of this study will focus on RPEG8CD3 and RPEG10CD4, which correspond closely to the optimum compositions.

2. Hydrogen-Bonding Interactions of the CDs in the Complex. Approximately two intramolecular hydrogen bonds per CD unit are obtained during the simulation, as shown in Table 2. The most important results in this table are the total number of intermolecular hydrogen bonds between CDs and the contribution of each pair of CDs. In support of the conclusion from Harada's group,[16,20] intermolecular hydrogen bonds between CDs are more numerous with HH sequences (5.8) than HT ones (3.7). The larger contribution to the total intermolecular hydrogen bonding for HH sequences comes for the head-to-head interaction (2.5• 2.7 hydrogen bonds for each of two head-to-head pairs).

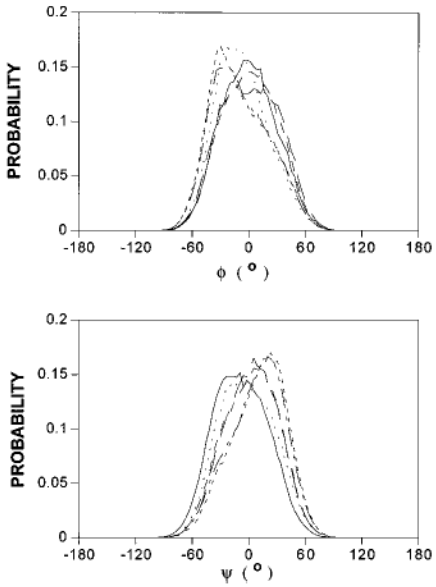

Figure 4. Distribution of six pairs of • and • at the bonds to the bridging oxygen atom for one of the CD units (number 2) for RPEG10CD4HH. The bridging oxygen atoms are displayed sequentially as (•) 1; (• •) 2; (• • •) 3; (- - -) 4; (•••) 5 and (- • - •) 6.

Tail-to-tail interactions gives a small contribution (0.6) to the number of intermolecular hydrogen bonds between CDs. The calculated binding energies slightly favor the HH sequences over the HT sequences (by 0.9 kcal/mol) in RPEG10CD4. Intermolecular hydrogen bonds from the interactions CD• PEG and CD• end group are less important.

3. Conformational Analysis of the CDs in the Complex. Bond Angles at the Bridging Oxygen Atoms. The values of the bond angles •, defined by C(1)• O• C(4′), are similar for all CDs. The average value, 117.8°, is close to the result of 117.7° for isolated CD and far from the value of 130.3° in the initial conformation of the polyrotaxanes.

Torsion Angles at the Bridging Oxygen Atom. The distribution function of • and • is depicted in Figure 4 for one of the CDs (number 2) in RPEG10CD4HH. Other CDs in the complex behave in a similar way. They show a single region of high probability for • and • , and this region includes the *trans* conformation. The shoulders in a few of the profiles, such as • at the second bridging oxygen atom, indicate that the profiles are the superposition of two overlapping distributions, each centered close to 0°. There is no indication of any population near the *cis* state at 180°.

In contrast to the result in Figure 4 for the CDs in the complex, • sometimes adopts a *cis* state in isolated CD.[30] This *cis* state is primarily responsible for the distortion of isolated cyclodextrins, where it orients the primary hydroxyl groups of two neighboring glucopyranose residues so that one OH group is blocking the cavity and the other one is oriented toward the outer cavity.[30] When the PEG chain fills the cavity, the *cis* state is inaccessible at • , and there is less distortion of the CD. CDs in the complex are more symmetric than isolated ones.

Torsion at C(5)• C(6). The torsion • is distributed over the three classic rotational isomeric states, g• , g• , and *trans*, as shown in Figure 5. Any of the • dihedral angles can visit all three states during the 0.5 ns MD simulation, as was also true for isolated CD.

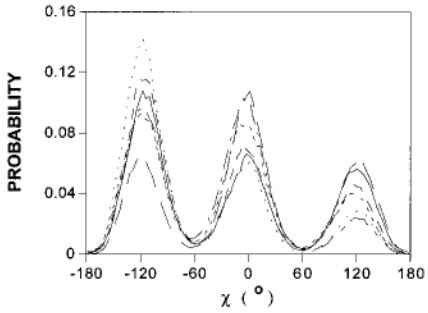

Figure 5. Distribution of • for one of the CD units (number 2) for RPEG10CD4HH. Torsional angles are displayed sequentially for glucopyranose units as (•) 1; (• •) 2; (• • •) 3; (- - -) 4; (•••) 5 and (-•-•) 6.

Table 3. Size, Shape, Distortion and Flexibility of Isolated • -CD and the Average of Four CDs in RPEG10CD4HH and RPEG10CD4HT[a]

parameters	• -CD[b]	RPEG10CD4HT	RPEG10CD4HH
$H_{initial}$, Å	8.81	8.81	8.81
$\langle H \rangle$, Å	6.59(0.40)	8.02(0.25)	8.06(0.26)
$R_{initial}$, Å	3.57	3.57	3.57
$\langle R \rangle$, Å	4.25(0.22)	4.17(0.35)	4.06(0.40)
$r_{initial}$, Å	3.55	3.55	3.55
$\langle r \rangle$, Å	3.35(0.38)	4.05(0.50)	4.06(0.47)
$V_{initial}$, Å^3	351	351	351
$\langle V \rangle$, Å^3	301(22)	434(84)	416(104)
• H^c	• 0.25(0.04)	• 0.09(0.03)	• 0.09(0.03)
• V^c	• 0.14(0.05)	0.24(0.24)	0.19(0.30)
• Torsion,[c] deg	101	45	46
$\langle s^2 \rangle^{1/2}$ (ring), Å	4.4	4.4	4.4
$\langle s^2 \rangle^{1/2}$ (head), Å	5.7	5.4	5.4
$\langle s^2 \rangle^{1/2}$ (tail), Å	5.0	5.5	5.5
• (*s*) (ring), Å	0.16	0.07	0.07
• (*s*) (head), Å	0.19	0.17	0.18
• (*s*) (tail), Å	0.36	0.38	0.37

[a] Standard deviations are in parenthesis. [b] From ref 28. [c] Parameters defined in the ref 30.

Cavity Size and Shape in the CDs. Table 3 collects the average of several parameters used to define the size of the cavities of the CDs, as well as the distortion and flexibility of the CD macrorings of isolated CD and two polyrotaxanes, RPEG10CD4HT and -HH. Column 2 has previous results for these parameters for isolated CD.[30] The table also shows *H*, *R*, *r* (defined in bottom of Figure 2), and V,

$$V \bullet \bullet H[rR \bullet (R^2 \bullet r^2)/3] \qquad (4)$$

for the nondistorted CD, in the conformation of the polyrotaxanes when the trajectory is initiated. These values were also used for the initial conformation in the analysis of isolated CDs.[30]

There is little difference in the parameters obtained for CD in polyrotaxanes HH and HT, but there are important differences between isolated CD and those forming part of either complex. The ratios $\langle r \rangle / \langle R \rangle$ are 0.79, 0.97, and 1.00 for isolated CD, RPEG10CD4HT, and RPEG10CDHH, respectively, showing that the cavities of the CDs in the complexes are more nearly cylindrical in shape. In contrast, for the isolated CD they were cone-shaped. Isolated CD shows an increase in the radius of the cavity on the side with the secondary hydroxyl groups ($\langle R \rangle$), a decrease in the radius of the cavity on the side of the primary hydroxyl groups ($\langle r \rangle$), and a considerable decrease in the height ($\langle H \rangle$) of the cone, compared with the values for the initial conformation. However, $\langle r \rangle$ and $\langle R \rangle$ of CDs in the complex increase and $\langle H \rangle$ decreases slightly. As a result, the

Table 4. End-to-End Distance, Radius of Gyration, and C_n for PEG*n* chain and Complexes RPEGnCDmHT and -HH

compound	$\langle r^2\rangle^{1/2}$, Å	$\langle s^2\rangle^{1/2}$, Å	C_n
PEG8	13	5.2	3.1
RPEG8CD3HT	27	7.6	14
RPEG8CD3HH	27	7.6	14
PEG10	14	5.9	3.1
RPEG10CD4HT	34	9.6	18
RPEG10CD4HH	34	9.6	18

volume of the cavity ($\langle V\rangle$) after equilibration is larger than in the initial nondistorted • -CD.

The parameters • *H*, • *V*, and • Torsion, which are the normalized change in depth, volume, and a cumulative magnitude of the changes in the torsion angles at the bridging oxygen atom,[30] describe the distortion of CDs. Due to the increase of $\langle H\rangle$ for CD in the complex relative to the isolated one, the absolute value of • *H* decreases when going from the isolated CD to the complex. The high values of $\langle r\rangle$, $\langle R\rangle$, and $\langle H\rangle$ for CD in the complex make • *V* positive. • Torsion are half of the values obtained for isolated CD. These results are a consequence of the more open and less distorted cavity when CD surrounds the PEG chain in the complex.

The root-mean-square radius of gyration was computed for three subsets of the oxygen atoms. These three subsets of $\langle s^2\rangle^{1/2}$ are for the 6 bridging oxygen atoms (ring), the 6 O6 oxygen atoms (tail), and the 12 secondary oxygen atoms O2 and O3 (head).[30] The results and their standard deviations • (*s*) are collected in the last rows of Table 3. Results for $\langle s^2\rangle^{1/2}$ support the conclusion in the previous paragraph. CDs in the complex are almost cylindrical. The width of the distribution • (*s*) (ring) gives a measure of the flexibility of the macroring. The low value (0.07) compared with the value for the isolated CD (0.16) shows that the flexibility of the macroring is now smaller. However, head and tail reflects a similar flexibility for isolated CDs or in the complex.

The parameters collected in Table 3 are averages of those obtained for each CD of the poly(rotaxanes). These parameters are very close for each of the four CDs in the complex; all CDs behave in a similar way. In general CDs in the complex have a cylindrical shape, and they increase their inner cavity volume to accomodate the polymer. Heights are similar to the ones obtained for nondistorted CDs. The distribution of the dihedral angles • and • , depicted in Figure 4, and the parameters • *H* and • Torsion, show that they are less distorted than the isolated CDs. From the analysis of the standard deviation • (*s*) (ring), CD macrorings are less flexible in the complex than the isolated CD, showing a more symmetric macroring structure than isolated CDs.

4. Conformation of PEG in the Complex. Radius of Gyration and End-to-End Distance. The radius of gyration and end-to-end distance have been computed for the isolated PEG chains, as well as those in the polyrotaxane complex. All non-hydrogen atoms of the chain, excluding the bulky end substituents, were taken into account for the radius of gyration. The end-to-end distance was calculated between nitrogen atoms directly bonded to the PEG chain. Table 4 shows the values for the complexes and the isolated PEG chains containing 8 and 10 ethylene oxide units with CDs. Characteristic ratios, defined as C_n • $\langle r^2\rangle/nl^2$, are collected in the last column of Table 4. The values for short isolated chains of 8 and 10 oxyethylene units are slightly less than the value of 5 expected for unperturbed chains with this number of bonds.[42] This result undoubtedly arises from the tendency for long flexible chains *in vacuo* to experience a coil• globular transition as the degree of polymerization increases.[43,44] The onset of this transition would be expected for PEG chains of about the size used here.

Table 5. Average Population (%) of the *trans* State for all Torsional Angles •$_1$ (O• CH_2• CH_2• O), •$_2$ (CH_2• CH_2• O• CH_2), and •$_3$ (CH_2• O• CH_2• CH_2) of the Isolated PEG*n* Chain and PEG in the RPEGnCDmHT and -HH Complexes

compound	•$_1$	•$_2$	•$_3$
PEG8	41	62	63
RPEG8CD3HT	92	83	83
RPEG8CD3HH	94	81	86
PEG10	45	59	64
RPEG10CD4HT	94	84	86
RPEG10CD4HH	94	85	84

The results show that the PEG chain expands when it forms the complex. The number of *trans* placements at C• C bonds is larger for PEG in the polyrotaxane complex than for isolated PEG, as we will see in the next section. This feature in the complexes is the origin of many experimental crystallographic characteristics of polyrotaxanes.

Dihedral Angles at Internal Bonds in the PEG Chain. The values of •$_1$, •$_2$, and •$_3$ were obtained for each of the *n* oxyethylene units of the chain for PEG*n* and RPEG*n*CD*m*. The CH_2• CH_2, CH_2• O, and O• CH_2 bonds have the three classical isomers g• , g• , and *trans*. The average of the population of the *trans* states over all bonds is collected in Table 5 for the isolated PEG chain and the PEG in RPEG*n*CD*m*, in the HT and HH forms. There is a larger population of *trans* states (and correspondingly smaller population of *gauche* states) in the complexes than in the isolated chain, by about a factor of 2.1 • 0.1 for •$_1$ at the C• C bond. For •$_2$ and •$_3$ this factor is approximately 1.3 • 0.1 and 1.6 • 0.3. The large increase for •$_1$ signifies that the "anomeric effect", invoked to explain the low population of the *trans* state at the C• C bond in unperturbed PEG,[45] is weakened in the complex.

Quantitative comparison of the distribution function for the dihedral angles was made using two properties deduced from the trajectories for each internal bond •$_{ix}$ (*i* • 1• 3) for the PEG chain: (a) the mean dihedral angle $\langle$••$_{ix}$ • •$_{trans}$•$\rangle$, where •$_{trans}$ is the dihedral angle for the *trans* placement, and (b) the fluctuation defined by

$$\bullet\bullet_{ix}\bullet\ \bullet_{trans}\bullet\bullet\ [\langle\bullet\bullet_{ix}\bullet\ \bullet_{trans}\bullet^2\rangle\bullet\ \langle\bullet\bullet_{ix}\bullet\ \bullet_{trans}\bullet\rangle^2]^{1/2} \quad (5)$$

Table 6 collects the averaged values over all internal bonds. As expected, values of both parameters are larger for the isolated chain PEG10 as compared to the PEG in the complex. The reasons are the larger population of *trans* states and the lower mobility of internal bonds for PEG chain in the complex, as compared to the isolated one. There is not much difference between results for complexes with HH or HT sequences of CDs.

Conclusions

Analysis of polyrotaxanes suggests that the isolated PEG chain captures as much CD as its length permits. The van der Waals interaction in PEG• CD is the main contribution to the stabilization of polyrotaxanes. Polyrotaxanes with CDs oriented head-to-head or tail-to-tail

Table 6. Averages of ⟨••$_i$• •$_{trans}$•⟩ and •••$_i$• •$_{trans}$• for the Internal Oxyethylene Units of Isolated PEG Chains and PEG in the Polyrotaxane Complexes

compound	angle, •$_i$	⟨••$_i$• •$_{trans}$•⟩, deg	•••$_i$• •$_{trans}$•, deg
PEG8	•$_1$	75	51
	•$_2$	50	68
	•$_3$	50	46
RPEG8CD3HH	•$_1$	22	28
	•$_2$	28	35
	•$_3$	28	36
RPEG8CD3HT	•$_1$	19	23
	•$_2$	30	38
	•$_3$	33	35
PEG10	•$_1$	72	52
	•$_2$	53	47
	•$_3$	52	48
RPEG10CD4HT	•$_1$	19	19
	•$_2$	27	34
	•$_3$	27	40
RPEG10CD4HH	•$_1$	19	24
	•$_2$	26	32
	•$_3$	24	32

are slightly more stable than those oriented head-to-tail due to intermolecular hydrogen-bonding interaction between CDs, with the larger contribution to the stabilization from intermolecular hydrogen bonds in the head-to-head or tail-to-tail arrangement. • -CDs in polyrotaxanes adopt a more symmetric macroring conformation, as compared to the isolated • -CDs. The *cis* states are totally suppressed at bonds to the bridging oxygen atom in the CDs in the complex. *Trans* states are strongly preferred at all the internal bonds of the PEG chain in the complex, in contrast to the well-known preference for *gauche* states at the C• C bond in unperturbed PEG. For this reason, the PEG in the complex is more extended than the unperturbed chain.

Acknowledgment. This research was supported by UAH-017/95 and DGICYT PB94-0364 and by National Science Foundation grant DMR 9523278.

References and Notes

(1) Bender, M. L.; Komillama, M. *Cyclodextrins Chemistry*; Springer Verlag: Berlin, 1978.
(2) Szejtli, J. *Cyclodextrin and Their Inclusion Complexes*; Akadémiai Kiadó: Budapest, 1982.
(3) Szejtli, J. *Cyclodextrins Technology*; Kluwer Academic Publishers: Dordrecht, 1988.
(4) Kohnke, F. H.; Mathias, J. P.; Stoddart, J. F. *Angew. Chem., Int. Ed. Engl. Adv. Mater.* **1989**, *28*, 1103.
(5) Anelli, P. L.; Ashton, P. R.; Ballardini, R.; Balzani, V.; Delgado, M.; Gandolfi, M. T.; Goodnow, T. T.; Kaifer, A. E.; Philip, D.; Pietraszkiewicz, M.; Prodi, L.; Reddington, M. V.; Slawin, A. N. Z.; Spencer, N.; Stoddart, J. F.; Vincent, C.; Williams, D. J. *J. Am. Chem. Soc.* **1992**, *114*, 193.
(6) Gibson, H. W.; Bhedda, M.; Engen, P. T.; Shen, Y. X.; Sze, J.; Wu, C.; Joardan, S.; Ward, T. C.; Lecavalier, P. R. *Makromol. Chem., Macromol. Symp.* **1991**, *42/43*, 395.
(7) Bergeron, R. J.; Channing, M. A.; Gibeily, G. J.; Pillor, D. M. *J. Am. Chem. Soc.* **1977**, *20*, 5146.
(8) Ogino, H. *J. Am. Chem. Soc.* **1981**, *103*, 1303.
(9) Ogino, H.; Ohata, K. *Inorg. Chem.* **1984**, *23*, 3312.
(10) Manka, J. S.; Lawrence, D. S. *J. Am. Chem. Soc.* **1990**, *112*, 2440.
(11) Venkata, T.; Rao, S.; Lawrence, D. S. *J. Am. Chem. Soc.* **1990**, *112*, 3614.
(12) Isnin, R.; Kaifer, A. E. *J. Am. Chem. Soc.* **1991**, *113*, 8188.
(13) Wenz, G.; Keller, B. *Angew. Chem. Int. Ed. Engl.* **1992**, *31*, 197.
(14) Harada, A.; Kamachi, M. *Macromolecules* **1990**, *23*, 2823.
(15) Harada, A.; Kamachi, M. *J. Chem. Soc., Chem. Commun.* **1990**, 1322.
(16) Harada, A. Li, J.; Kamachi, M. *Nature* **1992**, *356*, 325.
(17) Harada, A.; Li, J.; Nakamitsu, T.; Kamachi, M. *J. Org. Chem.* **1993**, *58*, 7524.
(18) Harada, A.; Li, J.; Kamachi, M. *Macromolecules* **1993**, *26*, 5698.
(19) Harada, A.; Li, J.; Kamachi, M. *J. Am, Chem. Soc.* **1994**, *116*, 3192.
(20) Harada, A.; Okada, M.; Li, J.; Kamachi, M. *Macromolecules* **1995**, *28*, 8406.
(21) McMullan, R. K.; Saenger, W.; Fayos, J.; Mootz, D. *Carbohydr. Res* **1973**, *31*, 37.
(22) Zhan, Y.; Mattice, W. L. *Macromolecules* **1992**, *25*, 4078.
(23) Haliloglu, T.; Mattice, W. L. *Macromolecules* **1993**, *26*, 3137.
(24) Zheng, N. R.; Mattice, W. L. *Acta Polym.* **1995**, *46*, 139.
(25) Dodge, R.; Mattice, W. L. *Macromolecules* **1991**, *24*, 2709.
(26) Zhan, Y.; Mattice, W. L. *J. Chem. Phys.* **1992**, *96*, 3279.
(27) Zhan, Y.; Mattice, W. L. *Macromolecules* **1992**, *25*, 3439.
(28) Lee, K.-J.; Mattice, W. L.; Snyder, R. G. *J. Chem. Phys.* **1992**, *96*, 9138.
(29) Tonelli, A. E. *Comput. Polym. Sci.* **1991**, *1*, 22.
(30) Pozuelo, J.; Madrid, J. M.; Mendicuti, F.; Mattice, W. L. *Comput. Theor. Polym. Sci.* **1996**, *6*, 125.
(31) Clark, M.; Cramer, R., III; Van Opdenbosch, N. *J. Comp. Chem.* **1989**, *10*, 982.
(32) Brant, D. A.; Flory, P. J. *J. Am. Chem. Soc.* **1965**, *87*, 663.
(33) Brant, D. A.; Flory, P. J. *J. Am. Chem. Soc.* **1965**, *87*, 2791.
(34) Goebel, C. V.; Dimpfl, W. L.; Brant, D. A. *Macromolecules* **1970**, *3*, 644.
(35) Goebel, K. D.; Brant, D. A. *Macromolecules* **1970**, *3*, 634.
(36) Brant, D. A.; Flory, P. J. *J. Am. Chem. Soc.* **1965**, *87*, 2788.
(37) Mattice, W. L.; Lo, J.-T. *Macromolecules* **1972**, *5*, 734.
(38) MOPAC-AM1. Included in the SYBYL 6.0 package.
(39) Abe, A.; Tasaki, K.; Mark, J. E. *Polym. J.* **1985**, *17*, 883.
(40) Verlet, L. *Phys. Rev.* **1967**, *159*, 98.
(41) Verlet, L. *Phys. Rev.* **1968**, *165*, 201.
(42) Allen, M. Tildesley, D. J. *Computer Simulation of Liquids*; Clarendon Press: Oxford, 1987.
(43) Tanaka, G.; Mattice, W. L. *Macromolecules* **1995**, *28*, 1049.
(44) Tanaka, G.; Mattice, W. L. *Macromol. Theory Simul.* **1996**, *5*, 499.
(45) Abe, A.; Mark, J. E. *J. Am. Chem. Soc.* **1976**, *98*, 6468.

MA961270Y